Emergence of Long-Range Order in $BaTiO_3$ from Local Symmetry-Breaking Distortions

M. S. Senn,[1,*] D. A. Keen,[2] T. C. A. Lucas,[3] J. A. Hriljac,[3] and A. L. Goodwin[1]
[1]Department of Chemistry, Inorganic Chemistry Laboratory, University of Oxford, South Parks Road, Oxford OX1 3QR, United Kingdom
[2]ISIS, Rutherford Appleton Laboratory, Harwell Campus, Didcot OX11 0QX, United Kingdom
[3]School of Chemistry, University of Birmingham, Edgbaston, Birmingham B15 2TT, United Kingdom
(Received 11 December 2015; published 20 May 2016)

By using a symmetry motivated basis to evaluate local distortions against pair distribution function data, we show without prior bias, that the off-center Ti displacements in the archetypal ferroelectric $BaTiO_3$ are zone centered and rhombohedral-like across its known ferroelectric and paraelectric phases. We construct a simple Monte Carlo model that captures our main experimental findings and demonstrate how the rich crystallographic phase diagram of $BaTiO_3$ emerges from correlations of local symmetry-breaking distortions alone. Our results strongly support the order-disorder picture for these phase transitions, but can also be reconciled with the soft-mode theory of $BaTiO_3$ that is supported by some spectroscopic techniques.

DOI: 10.1103/PhysRevLett.116.207602

The phenomenological study of displacive phase transitions by the Landau-Ginzburg theory has been exceptionally fruitful [1]. Its apparently close relationship to the theory of soft-mode phase transitions [2,3] has meant that the expansion of the free energy of a system in terms of the correct order parameter can lead to a one-to-one correspondence with the energy of a phonon mode in the harmonic approximation. Studies of global lattice and electronic instabilities benefit from the classification of global symmetry breaking (an order parameter) in terms of irreducible representations (see Ref. [4] and references therein) of the parent symmetry space, which themselves have a correspondence with the eigenvectors (harmonic phonons) of the system. Furthermore, their allowed couplings (or phonon-phonon scatterings) may be studied up to a given order by considering only those that are invariant under the parent symmetry operators [5]. This, combined with the fact that global symmetry dictates both microscopic structure and macroscopic observables in these phase transitions means that the latter, which are often more conveniently measured, may be used as the order parameter for these phase transitions. However, many macroscopic observables are a result of emergent phenomena driven by local ordering, which combine in often counterintuitive ways to produce the global symmetry of the structure. Hence, the local symmetry effectively controls the physical property [6]. Here, a phenomenological model based around a macroscopic (or crystallographic) parameter will not lead to a valid physical insight into the phase transition. Hence, microscopic studies of local symmetry breaking are vital if physical understanding is to be gained.

In any crystallographic model there are many ways to locally break the average symmetry, for example, through thermal effects, distortions, or dislocations. The difficulty is to coalesce these local degrees of freedom into an understandable form within a given length scale and to evaluate their contribution systematically against data sensitive to local correlations such as x-ray absorption near edge structure (XANES), EXAFS, the pair distribution function (PDF), and diffuse scattering. It is particularly desirable to compare against neutron PDF data, which are sensitive to local distortions beyond a length scale of the first coordination shell. As no simple method exists for doing this, often our understanding of emergent phenomena in condensed phases is based on model building biased towards the macroscopic observables, whereas ideally these properties should emerge spontaneously from our analysis of the local structure. Here, we present such a method and demonstrate its effectiveness at identifying the local order parameter in $BaTiO_3$. This provides the first unbiased local model of this system and shows how the crystallographic phase transitions can emerge naturally from the correlations of the local symmetry-breaking distortions.

The ferroelectric properties of $BaTiO_3$ were first reported in the 1940s [7]. The ferroelectricity and concomitant cubic to tetragonal structural distortion [8] were initially discussed in the framework of displacive phase transitions [9]. However, the subsequent observations of orthorhombic and rhombohedral phase transitions at lower temperatures [10,11] are inconsistent with second-order displacive phase transitions. This anomaly together with the observation of diffuse x-ray scattering in all but the low temperature rhombohedral phase [12] led to the development of the phenomenological order-disorder model [13]. This has been supported by other techniques sensitive to local order such as PDF [14] and XANES or EXAFS methods [15]. In this model, the incipient

ferroelectric displacements of the Ti are taken to be rhombohedral-like, towards the faces of the TiO_6 octahedra [Fig. 2(b)], with long-range correlations in chains along ⟨100⟩, and disorder between chains giving rise to the average crystallographic symmetry. The model explains the sheets of diffuse x-ray scattering observed in isostructural $KNbO_3$ [13] and removes the requirement for the phase transitions to proceed via group-subgroup relationships. However, diffuse scattering data have been analyzed in terms of soft phonon modes [16] and many spectroscopic techniques such as Raman [17,18] and inelastic neutron [19,20] scattering still appear to support a displacive phase transition model. Additionally, it has been shown computationally that the cubic to tetragonal phase transitions can be achieved by combining features of order-disorder and displacive type mechanisms [21]. Clearly, consensus in the research community has yet to be reached.

Polycrystalline $BaTiO_3$ was prepared by conventional solid state synthesis. A 2 cm^3 sample was loaded into an 8 mm diameter cylindrical vanadium can, and neutron powder diffraction data were collected at 500, 410, 350, 293, 250, 210, 150, and 15 K on the instrument GEM [22] at ISIS, UK. The maximum usable Q was 40 $Å^{-1}$ and counting times were 6–8 h. Rietveld refinements were performed in TOPAS. The total scattering data were corrected for background, sample container, multiple scattering, absorption, and inelasticity effects using Gudrun [23] to produce the real-space PDF. As we are performing our fitting procedure in PDFFit [24] we work here with $G^{\mathrm{PDF}}(r)$, which is proportional to $D(r)$ and whose relationship with other parametrizations of the PDF is given in Ref. [25].

Although visual differences are evident in the PDFs as a function of temperature (Fig. 1), modeling is required to extract the local distortions of the atoms from their high symmetry positions. Two approaches exist; one is a small box method fitting the data while relying on a crystallographic unit cell akin to Rietveld fitting (e.g.. Ref. [26]) and the other is a big box method where a large supercell is refined using reverse Monte Carlo (RMC) calculations [27]. The problem with conventional small box PDF analysis is that the parametrization requires an *a priori* assumption of the nature of the local distortions. Equally, in RMC refinements, where the degrees of freedom are many, there are many ways to interrogate the refined parameters and an exhaustive analysis is impractical; bias is often introduced at this stage. Recent work [28] has sought to tackle this problem by decomposing RMC configurations in terms of their zone center irreducible representations (irreps). However, short range correlations beyond this length scale are lost in this analysis, and the modeling or refinement stage does not make use of the inherent orthogonality of symmetry adapted displacements. In contrast, the method we use here involves

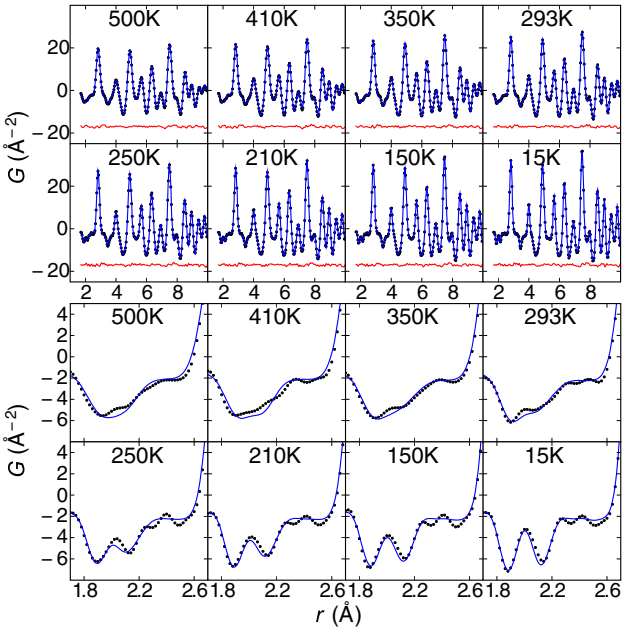

FIG. 1. Fits to $G(r)$ at the various temperatures indicated using symmetry-adapted displacements belonging to the Γ_4^- irrep only. The enlarged region around 1.8–2.2 Å shows the Ti-O bonds, which change most visibly as a function of temperature. The fitting procedure is described in the text.

expanding the degrees of freedom of the crystallographic unit cell up to a given supercell size in terms of both zone center and zone boundary irreps of the "parent" space group. The collection of symmetry-breaking displacements transforming as the same irrep may be further decomposed into symmetry-adapted distortion modes (hereafter referred to simply as modes). A number of web based tools can perform this decomposition [29,30] and this parametrization has been used successfully in Rietveld refinement to systematically test for symmetry breaking during phase transitions [31,32]. We extend this further by utilizing the constraint language of PDFGui and PDFFit [24] to refine mode amplitudes directly against PDF data. Further details of the implementation are given as Supplemental Material [33] and a comprehensive description will be published elsewhere.

Figure 1 shows best fits from our data analysis procedure at each temperature. We obtain very good fits to all the PDF data, with differences between the observed and calculated intensities being of the order of the Fourier ripples in the data. Of course, the parametrization of the xyz degrees of freedom into modes does not change the overall goodness of fit but merely facilitates a systematic search of all parameter space. In the Supplemental Material [33] we also show that these fits are superior to those obtained with a big box RMC type model (noting that RMC models are also constrained to simultaneously fit the Bragg profile) and that average models from Rietveld analysis are inadequate at describing the PDF data at all but the lowest temperatures.

We performed the analysis on a $2 \times 2 \times 2$ $P1$ supercell of the $Pm\bar{3}m$ unit cell of paraelectric $BaTiO_3$, which encompasses all of the common symmetry lowering phase transitions observed in the perovskite family leading to 120 internal degrees of freedom, although our analysis can easily be extended to incorporate displacements with longer period modulations. We chose this supercell size to be appropriate to tackle many other order-disorder phase transitions in perovskites, and to test whether the ferroelectric modes may have zone-boundary character as suggested by a recent theoretical study [36]. We systematically tested the modes (by irrep) against Bragg and PDF data separately to emphasize when local and global symmetries agree or diverge. Each PDFFit or Rietveld refinement was initiated from random starting values 500 times at each temperature to ensure that global minima were reached. Modes with vanishingly small refined amplitudes, or which produced poor fits, cannot be significant order parameters. In Fig. 2 for each set of modes belonging to an irrep tested in turn, we plot a weighted average of the refined mode magnitudes. The weighting is such that large magnitudes from poorly fitting refinements corresponding to false minima have a vanishing contribution to the average through a Boltzmann distribution $\exp[(Rw_{\text{global}} - Rw)/\sigma]$. We call this quantity the Boltzmann weighted mean amplitude (BWMA). Rw_{global} is the minimum value obtained in all refinements of the weighted R factor with $\sigma = 0.1\%$. The value of σ is chosen such that two fits differing by this amount may only just be visually discriminated. Triply degenerate modes in the cubic symmetry corresponding to equivalent distortions in the x, y, and z directions are averaged together for these plots. The distortion mode BWMAs have three distinct types of behavior: (1) low values at 500 K rising to large values at lower temperatures, (2) small values at 500 K dropping to near zero, and (3) consistently near zero values.

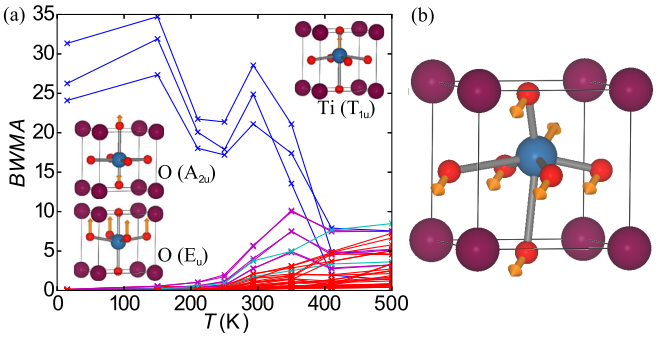

FIG. 2. (a) BWMAs from PDF refinements for all modes plotted against temperature. Modes belonging to Γ_4^-, X_5^+, M_2^-, and all other irreps are colored blue, magenta, cyan, and red respectively. Insets show symmetry-adapted displacements belonging to the Γ_4^- irrep, which correspond to the three modes with the highest BWMA values and (b) shows their combined $+--$ coupling [$\text{Ti}(T_{1u})$, $\text{O}(A_{2u})$, and $\text{O}(E_u)$, respectively] along the rhombohedral order parameter direction as observed locally in this study at all temperatures.

Modes of type (1) are clearly the relevant order parameters for the ferroelectric phase transitions. These modes all belong to the Γ_4^- irrep and correspond to nine degrees of freedom, three branches each for the $\text{Ti}(T_{1u})$, $\text{O}(A_{2u})$, and $\text{O}(E_u)$ modes. Since modes belonging to different irreps are necessarily orthogonal and do not couple (in the harmonic approximation), we need not test for inter-irrep correlations, but instead can focus on intra-irrep correlations within the basis describing the distortion space spanning this Γ_4^- irrep. Analysis of the three branches of each of these modes reveals that the order parameter always has rhombohedral symmetry from the local perspective, whereas our analysis of the Bragg profile in terms of global (crystallographic) symmetry follows the well known cubic, tetragonal, orthorhombic, and rhombohedral phase transitions described in the literature. Full details of the order parameter direction at all temperatures are given in the Supplemental Material [33]. Our results are consistent with recent RMC refinements on the tetragonal phase of $BaTiO_3$, which find a Ti distribution in agreement with a picture of local rhombohedral-like distortions [37]; however, the clear off-center nature of the Ti distributions that we observe, is not so evident in that work. Case (2) demonstrates our sensitivity to soft phonon modes. These belong to the irrep. X_5^+ or M_2^-, are soft eigenvectors of the system [38], and are on the same line in the phonon dispersion curves as the zone centered Γ_4^- ferroelectric instability, such that they both correspond to locally the same off-center distortions, but are antiferroelectric in nature. Case (3) shows that a large number of modes do not have a significant contribution to describing the local symmetry breaking distortions in $BaTiO_3$.

The origin of the local order parameter is a strong desire for Ti to undergo a second order Jahn-Teller distortion, presumably driven by a hybridization of the oxygen $2p$ orbitals with the Ti $3d$ orbitals [39] by shortening three bonds simultaneously, i.e., a local rhombohedral-like distortion. The incipient rhombohedral distortions are necessarily split by global tetragonal and orthorhombic lattice distortions at particular temperatures, and the question now arises, can these lattice distortions themselves be a result of correlations of the local symmetry-breaking distortions alone? Or put another way, can this order-disorder model provide a complete description of the observed phase transitions in $BaTiO_3$?

To test this we perform a Monte Carlo (MC) simulation using a simple model Hamiltonian. We do not claim that this represents the true physical Hamiltonian of the system, but use it to show that local coupling of Ti displacements can reproduce the observed series of crystallographic phase

transitions and is consistent with previously reported diffuse scattering [13]. The Hamiltonian is of the form

$$\mathcal{H} = J_1 \sum_{\langle\langle i,j \rangle\rangle} \delta\left[\frac{\sqrt{3}}{2\sqrt{2}}(\mathbf{S}_i^{\parallel} - \mathbf{S}_j^{\parallel}) - \hat{\mathbf{r}}_{ij}\right] + J_2 \sum_{\langle\langle\langle i,j \rangle\rangle\rangle} \left[\delta(\mathbf{S}_i - \hat{\mathbf{r}}_{ij}) \times \delta\left(\mathbf{S}_j \cdot \hat{\mathbf{r}}_{ij} + \frac{1}{3}\right)\right] + J_3 \sum_{\langle i,j \rangle} \mathbf{S}_i \cdot \mathbf{S}_j.$$

$\mathbf{S}_i$ denotes the normalized displacement vector of Ti site i and $\hat{\mathbf{r}}_{ij}$ the normalized vector joining sites i and j. The coupling parameters have J_1, $J_2 > 0$, $J_3 < 0$, and $|J_3| < |J_2| < |J_1|$. $\langle i, j\rangle$ denotes a sum over nearest-neighbor sites i, j; double and triple angle brackets denote sums over second and third nearest neighbors, respectively. The three terms in this toy Hamiltonian penalize dipole misalignment in first-, second-, and third-nearest neighbor sites as shown in the inset of Fig. 3(a). This Hamiltonian is the cost function for a MC simulation with a $10 \times 10 \times 10$ supercell in which all dipoles are hard wired to have a common projection along any one chain when viewed down one of the $\langle 100\rangle$ directions [i.e., we assume a J_0 term with high energy in keeping with Ref. [13] and as illustrated in the inset of Fig. 3(a)]. The simulation [Fig. 3(a)] shows three distinct phase transitions with discontinuities in the macroscopic polarization. In Figs. 3(b)–3(e) we illustrate portions of representative configurations of the correlated disorder in the MC simulation, along with their calculated diffuse scattering. Both our calculated diffuse scattering and observed chainlike configurations of off-center Ti displacements are consistent with those published earlier [12,13].

These MC simulations show how the observed sequence of phase transitions can arise from local correlations of nearest-neighbor type interactions alone and strongly support the order-disorder picture of $BaTiO_3$. Importantly, this order-disorder picture is not necessarily contradictory to spectroscopic results and a soft-mode picture [17–20]. When our high temperature cubic phase is viewed down any of its fourfold axes, the correlated disorder of the Ti displacements clearly has average tetragonal symmetry. There are six symmetry equivalent tetragonal-like chains, for each of which the average of the Ti displacements lies along one of the $\langle 100\rangle$ directions. A spontaneous symmetry-breaking event in which an interchain correlation length tends to infinity could be viewed as a pseudotetragonal soft mode phase transition. Indeed, diffuse scattering associated with the cubic to tetragonal phase transition has been shown to be equally well described by soft mode models [40,41], which are relatively dispersionless in nature [42]. The present work hence provides a microscopic justification for why this duality in the description of the diffuse scattering exists.

Our results are the first unbiased determination of local symmetry in $BaTiO_3$ across all its known phases. They show that local displacements of the Ti atoms are zone centered and

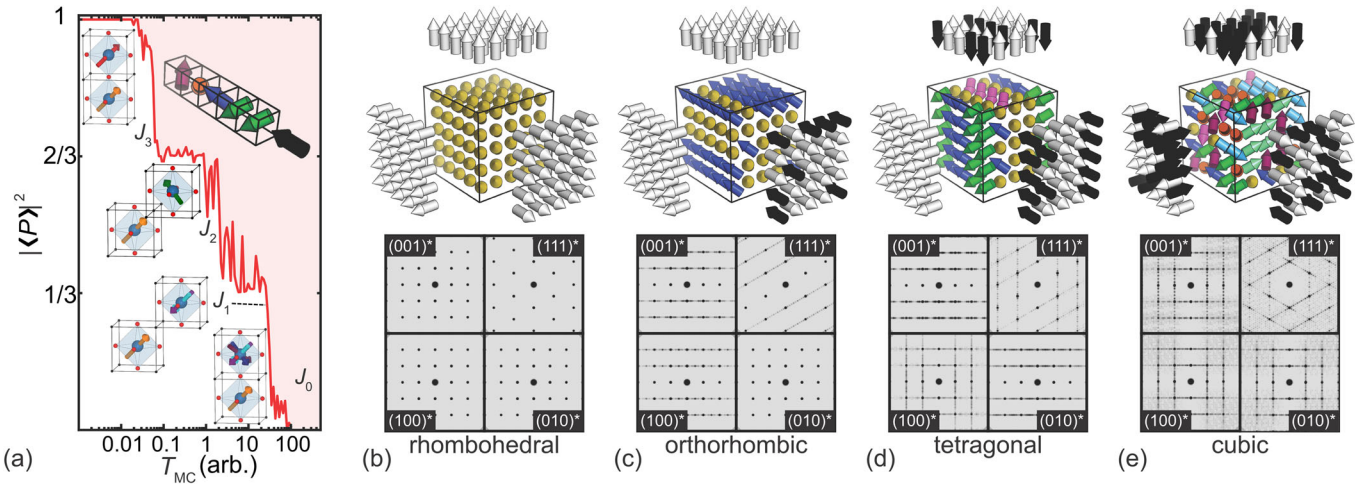

FIG. 3. (a) MC simulation reproducing the tetragonal, orthorhombic, and rhombohedral phase transitions, with the square of the average polarization serving as an order parameter. Insets below the polarization line identify the relevant interactions penalized by our Hamiltonian, placed at temperatures where their energy scales become important in the simulation; above the line is a representation of the chainlike correlations present in the cubic phase (J_0, hardwired into our simulations) showing how the projection of the polarization along the direction of a chain is always preserved (black arrow). (b)–(e) A portion of a MC configuration for each phase, with the polar vector projections along the $\langle 100\rangle$ directions, and the calculated diffuse scattering in the planes indicated. It is the interchain disorder between the polar vector projections (white and black arrows) that gives rise to diffuse planes of scattering in reciprocal space. In the cubic phase it is in all three $\langle 100\rangle$ directions, giving three sets of intersecting orthogonal diffuse scattering planes in reciprocal space, and each successive phase transition represents interchain orderings along successive $\langle 100\rangle$ directions. An enlarged version of this figure is given as part of the Supplemental Material [33].

rhombohedral-like at all temperatures. The fact that a simple Hamiltonian, which considers only local interactions, can reproduce the rich phase diagram in a MC simulation gives strong support to the order-disorder picture for $BaTiO_3$ and demonstrates how global symmetry may emerge from local symmetry-breaking distortions. This fundamental insight highlights the importance of our methodology for determining local symmetry in order-disorder phase transitions and demonstrates its power when it is coupled to MC simulations. We note that recent developments in speeding up the simulation of PDF data by orders of magnitude [43] will allow the exploration of ever more complicated systems exhibiting order-disorder phase transitions, and hope that our work will stimulate research into a host of other systems exhibiting emergent phenomena.

We would like to acknowledge STFC for awarding us neutron beam time. M. S. S. is grateful to the Royal Commission for the Exhibition of 1851 for the support of a fellowship, A. L. G for funding from the ERC (Grant No. 279705), and T. C. A. L. and J. A. H. for studentship funding from Diamond Light Source.

*mark.senn@chem.ox.ac.uk

[1] R. A. Cowley, Adv. Phys. **29**, 1 (1980).
[2] P. Sollich, V. Heine, and M. T. Dove, J. Phys. Condens. Matter **6**, 3171 (1994).
[3] M. T. Dove, A. P. Giddy, and V. Heine, Ferroelectrics **136**, 33 (1992).
[4] H. T. Stokes, B. J. Campbell, and R. Cordes, Acta Crystallogr. Sect. A **69**, 388 (2013).
[5] D. M. Hatch and H. T. Stokes, J. Appl. Crystallogr. **36**, 951 (2003).
[6] D. A. Keen and A. L. Goodwin, Nature (London) **521**, 303 (2015).
[7] A. Von Hippel, R. G. Breckenridge, F. G. Chesley, and L. Tisza, Ind. Eng. Chem. **38**, 1097 (1946).
[8] H. D. Megaw, Proc. R. Soc. A **189**, 261 (1947).
[9] W. Cochran, Adv. Phys. **9**, 387 (1960).
[10] H. F. Kay and P. Vousden, Philos. Mag. **40**, 1019 (1949).
[11] R. G. Rhodes, Acta Crystallogr. **2**, 417 (1949).
[12] R. Comès, M. Lambert, and A. Guinier, Solid State Commun. **6**, 715 (1968).
[13] R. Comès, M. Lambert, and A. Guinier, Acta Crystallogr. Sect. A **26**, 244 (1970).
[14] G. H. Kwei, S. J. L. Billinge, S.-W. Cheong, and J. G. Saxton, Ferroelectrics **164**, 57 (1995).
[15] B. Ravel, E. A. Stern, R. I. Vedrinskii, and V. Kraizman, Ferroelectrics **206**, 407 (1998).
[16] M. Holma, N. N. Takesue, and H. Chen, Ferroelectrics **164**, 237 (1995).
[17] L. Rimai, J. L. Parsons, and J. T. Hickmott, Phys. Rev. **168**, 623 (1968).
[18] H. Vogt, J. A. Sanjurjo, and G. Rossbroich, Phys. Rev. B **26**, 5904 (1982).
[19] G. Shirane, B. Frazer, V. Minkiewicz, J. Leake, and A. Linz, Phys. Rev. Lett. **19**, 234 (1967).
[20] G. Shirane, J. D. Axe, and J. Harada, Phys. Rev. B **2**, 3651 (1970).
[21] R. Pirc and R. Blinc, Phys. Rev. B **70**, 134107 (2004).
[22] P. Day, J. Enderby, W. Williams, L. Chapon, A. C. Hannon, P. Radaelli, and A. K. Soper, Neutron News **15**, 19 (2004).
[23] S. E. McLain, D. T. Bowron, A. C. Hannon, and A. K. Soper, GUDRUN, a computer program developed for analysis of neutron diffraction data, Chilton, ISIS Facility, Rutherford Appleton Laboratory, 2012.
[24] C. L. Farrow, P. Juhas, J. W. Liu, D. Bryndin, E. S. Božin, J. Bloch, T. Proffen, and S. J. L. Billinge, J. Phys. Condens. Matter **19**, 335219 (2007).
[25] D. A. Keen, J. Appl. Crystallogr. **34**, 172 (2001).
[26] S. J. L. Billinge, Z. Kristallogr. **219**, 117 (2004).
[27] H. Y. Playford, L. R. Owen, I. Levin, and M. G. Tucker, Annu. Rev. Mater. Res. **44**, 429 (2014).
[28] J. R. Neilson and T. M. McQueen, J. Appl. Crystallogr. **48**, 1560 (2015).
[29] B. J. Campbell, H. T. Stokes, D. E. Tanner, and D. M. Hatch, J. Appl. Crystallogr. **39**, 607 (2006).
[30] J. M. Perez-Mato, D. Orobengoa, and M. I. Aroyo, Acta Crystallogr. Sect. A **66**, 558 (2010).
[31] B. J. Campbell, J. S. O. Evans, F. Perselli, and H. T. Stokes, IUCr Comput. Comm. Newsl. **8**, 81 (2007).
[32] S. Kerman, B. J. Campbell, K. K. Satyavarapu, H. T. Stokes, F. Perselli, and J. S. O. Evans, Acta Crystallogr. Sect. A **68**, 222 (2012).
[33] See Supplemental Material at http://link.aps.org/supplemental/10.1103/PhysRevLett.116.207602, which includes Refs. [34,35], for details of the symmetry adapted distortion mode parameterization, Rietveld and PDF refinement results and analysis of the order parameter directions.
[34] A. A. Coelho, Topas (2009); http://www.topasacademic.net/.
[35] J. S. O. Evans, Mater. Sci. Forum **651**, 1 (2010).
[36] Q. Zhang, T. Cagin, and W. A. Goddard, Proc. Natl. Acad. Sci. USA **103**, 14695 (2006).
[37] I. Levin, V. Krayzman, and J. C. Woicik, Phys. Rev. B **89**, 024106 (2014).
[38] P. Ghosez, X. Gonze, and J. P. Michenaud, Ferroelectrics **206**, 205 (1998).
[39] R. E. Cohen, Nature (London) **358**, 136 (1992).
[40] N. L. Matsko, E. G. Maksimov, and S. V. Lepeshkin, J. Exp. Theor. Phys. **115**, 309 (2012).
[41] A. Hüller, Solid State Commun. **7**, 589 (1969).
[42] E. Farhi, A. Tagantsev, R. Currat, B. Hehlen, E. Courtens, and L. Boatner, Eur. Phys. J. B **15**, 615 (2000).
[43] A. A. Coelho, P. A. Chater, and A. Kern, J. Appl. Crystallogr. **48**, 869 (2015).